Functionally Graded Cathodes for Solid Oxide Fuel Cells

Final Report

Reporting Period Start Date: October 1, 2002

Reporting Period End Date: April 30, 2008

Principal Authors
Lei Yang, Ze Liu, Shizhong Wang, Jaewung Lee, and Meilin Liu

Report Issued: July 29, 2008

DOE Contract No.: DE-FC26-02NT41572

Center for Innovative Fuel Cell and Battery Technologies
School of Materials Science and Engineering
Georgia Institute of Technology
Atlanta, GA 30332-0245

DISCLAIMER

ABSTRACT

The main objective of this DOE project is to demonstrate that the performance and long-term stability of the state-of-the-art LSCF cathode can be enhanced by a catalytically active coating (e.g., LSM or SSC).

We have successfully developed a methodology for reliably evaluating the intrinsic surface catalytic properties of cathode materials. One of the key components of the test cell is a dense LSCF film, which will function as the current collector for the electrode material under evaluation to eliminate the effect of ionic and electronic transport. Since it is dense, the effect of geometry would be eliminated as well.

From the dependence of the electrode polarization resistance on the thickness of a dense LSCF electrode and on partial pressure of oxygen, we have confirmed that the surface catalytic activity of LSCF limits the performances of LSCF-based cathodes. Further, we have demonstrated, using test cells of different configurations, that the performance of LSCF-based electrodes can be significantly enhanced by infiltration of a thin film of LSM or SSC. In addition, the stability of LSCF-based cathodes was also improved by infiltration of LSM or SSC.

While the concept feasibility of the electrode architecture is demonstrated, many details are yet to be determined. For example, it is not clear how the surface morphology, composition, and thickness of the coatings change under operating conditions over time, how these changes influence the electrochemical behavior of the cathodes, and how to control the microscopic details of the coatings in order to optimize the performance. The selection of the catalytic materials as well as the detailed microstructures of the porous LSCF and the catalyst layer may critically impact the performance of the proposed cathodes.

Further, other fundamental questions still remain; it is not clear why the degradation rates of LSCF cathodes are relatively high, why a LSM coating improves the stability of LSCF cathodes, which catalysts would be most effective for LSCF, and how to achieve further enhancement of the performance and stability of SOFC cathodes.

TABLE OF CONTENTS

LIST OF GRAPHICAL MATERIALS

INTRODUCTION

The cathode is an important area of SOFC development since most of the cell power losses arise in the cathode, more so at lower operating temperatures. One of the reasons that $La_xSr_{1-x}Co_yFe_{1-y}O_{3-\delta}$ (LSCF) shows much better performance than LSM is because LSCF has much higher ionic and electronic conductivity than LSM, extending the active sites beyond the TPBs to the entire surface of the LSCF.[1-3] One obvious downfall for LSCF is that it reacts adversely with YSZ, which can be mitigated by the use of a buffer layer of doped-CeO_2 between LSCF and YSZ.[4] However, the catalytic activity of the stand-alone LSCF cathodes is likely to be limited by the surface catalytic properties. Further, the long-term stability of LSCF cathodes is a concern [5-6]. Thus, it is hypothesized that the *performance* and *stability* of a porous LSCF cathode may be improved by the application of a catalytically active coating though infiltration.[7] The selection of the catalytic materials as well as the detailed microstructures of the porous LSCF and the catalyst layer may critically impact the performance of the proposed cathodes.

The main objective of this project is to determine if the stability and/or catalytic properties (or the performance) of porous LSCF cathodes can be further enhanced by infiltration of other catalytically active materials (such as LSM and SSC). More specifically, the technical objectives include

- To develop a strategy for reliable testing of surface catalytic properties of a thin film cathode material without the limitation of sheet resistance;
- To determine the effect of surface modification of porous LSCF (by infiltration of another catalyst) on the area-specific polarization resistance;
- To perfect processing procedures for fabrication of test cells with LSCF electrodes of controlled density/porosity, thickness, morphology, and performance;
- To determine the optimal thickness of LSCF and coatings by sputtering; and
- To evaluate stability over time (~100 hours testing).

Since the performance of SOFCs depends sensitively on the performance of the cathodes (more so at lower operating temperatures), reduction in cathode polarization resistance and improvement in stability by infiltration of catalytically active coatings will ultimately reduce the cost of SOFC technology and help to meet DOE cost goals.

EXECUTIVE SUMMARY

The objective of this project is to determine if the *stability* and/or *catalytic properties* (or the performance) of porous LSCF cathodes can be further enhanced by infiltration of other catalytically active materials, to investigate the effect of surface modification of porous LSCF (by infiltration of another catalyst) on the area-specific polarization resistance, and to evaluate stability of infiltrated cathodes under typical SOFC testing conditions [8].

The approach is to modify the surface of a porous LSCF backbone (having high ionic and electronic conductivity) by a thin coating of LSM or SSC (having high stability and catalytic activity toward O_2 reduction). The novelty of our cathodes is in the selection and the detailed microstructure of materials that create a better performing cathode. The hypothesis is that the performance of such a cathode can be enhanced by either improving the transport properties of the backbone or the catalytic activity of the catalyst, or both. The uniqueness of this approach is to integrate materials of different properties and make the best use of them. Since LSCF has excellent ionic the electronic conductivity, the performance of stand-alone LSCF cathodes is likely limited by the surface catalytic activity. Thus, infiltrating a porous LSCF backbone with a catalytically active coating material to enhance the catalysis of oxygen reduction at the gas-solid interface should further enhance the performance of the cathodes.

The main accomplishments can be briefly summarized as follows

- Designed a unique test cell configuration for determining the surface catalytic properties of candidate infiltration catalysts
- Fabricated high quality thin films of cathode materials for evaluating their intrinsic catalytic activities
- Demonstrated that the surface activity of LSCF can be improved by infiltration of suitable catalysts
- Demonstrated that the stability of LSCF cathodes can be improved by infiltrated of a thin LSM or SSC.

In addition to LSM and SSC examined in the feasibility study, other catalytically more active catalysts (to replace LSM and SSC) and more conductive matrixes or backbones (to replace LSCF) are yet to be identified or developed for further enhancement of the performance and stability of SOFC cathodes.

While the concept feasibility of the electrode architecture is demonstrated, many details are yet to be determined. For example, it is not clear how the surface morphology, composition, and thickness of the coatings change under operating conditions, how these changes influence the electrochemical behavior of the cathodes, and how to control the microscopic details of the coatings in order to optimize the performance.

EXPERIMENTAL

To achieve the project objectives, we perform the following tasks:

Task 1 – Demonstrate a strategy for reliable testing of surface catalytic properties of a thin film cathode material with minimal errors. This includes the design and fabrication of a testing apparatus as well as testing cells to minimize or eliminate the effect of sheet resistance, the interference of current collectors, and other extrinsic factors that may compromise the consistency of performance evaluation.

Task 2 – Demonstrate the effect of surface modification of LSCF (by sputtering of another catalyst) on the area-specific polarization resistance. To demonstrate the concept feasibility, we started with electrolyte substrates followed by sputtering a dense layer of LSCF and then another dense layer of LSM or SSC. The main advantage of this test cell over conventional cells with porous electrodes is to leave out the complex effects of microstructure on cell performance.

Task 3 – Develop processing procedures for fabrication of test cells with porous LSCF electrodes. Porous LSCF backbones will be screen-printed on GDC electrolyte substrates and fired to ~1080°C in order to bond the LSCF to the electrolyte. We will then infiltrate the LSM or SSC, permuting precursor loading and firing temperature in order to produce different infiltrated microstructures. This includes optimizing the infiltration process to establish control of the wetting, thickness, and morphology of infiltrated catalysts (LSM or SSC), and a regime of testing to determine what infiltrated procedures work best.

Task 4 – Determine the optimal thicknesses of LSCF and LSM or SSC coatings using cells with electrodes of well controlled thickness and density (by sputtering). The thickness of the LSCF and LSM or SSC will be systematically varied to optimize the performance. We will test the performance of these cells using impedance at open circuit and under load against LSCF electrodes without surface modification. The microstructure, morphology, and phases of the electrodes will be characterized using SEM and XRD before and after electrochemical performance testing to determine which morphologies give the best performance.

Task 5 – Determine performance and microstructure stability of anode-supported cells over time (~4 days or ~100 hours testing).

Task 6 – Evaluate the effect of a thin-film YSZ coating on the performance of an LSCF cathode.

The samples tested in this project are summarized in the table below:

		Cell configuration	Other details
A.	**Test cells with dense electrodes by sputtering**		
	A1.	Pt mesh/Porous LSCF| GDC | dense LSCF	Thickness of dense LSCF: 150 nm, 250nm, 400nm, 550nm, 750 nm, 1000nm,
	A2.	Pt mesh/Porous LSCF| GDC | dense LSCF/dense LSM	LSCF: 1000nm; LSM: 5nm, 10nm, 20nm
	A3.	Pt mesh/Porous LSCF| GDC | dense LSCF/dense SSC	
	A4.	Pt mesh/Porous LSCF| GDC | dense LSCF/a thin YSZ	LSCF: 1000nm; YSZ: discontinuous film(sputter 10 seconds)
B.	**Symmetrical cells with porous LSCF**		
	B1.	Porous LSCF | GDC | Porous LSCF (blank cell without infiltration)	LSCF: screen printing/ brush painting; porosity—20-40%; thickness—~30 μm; grain size—0.3-0.8μm
	B2.	Porous LSCF | GDC | Porous LSCF (blank cell with LSCF infiltration)	0.48mol/L LSCF infiltration: nano particle—50-100nm
	B3.	Porous LSCF | GDC | Porous LSCF (blank cell with LSM infiltration)	0.0156mol/L, 0.0312mol/L, 0.0625mol/L, 0.125mol/L, 0.25mol/L LSM infiltration LSM in LSCF backbone: nano particle—5-15nm; thickness—~20nm
	B4.	Porous LSCF | GDC | Porous LSCF (blank cell with SSC infiltration)	0.0625mol/L, 0.16mol/L 0.48mol/L, 1.44mol/L SSC infiltration SSC in LSCF backbone: nano particle—50-100nm; thickness—~60nm
C.	**Anode-supported cells (Home-Made)**		
	C1.	Ni-GDC | GDC | porous LSCF (blank cell without infiltration)	Ni-GDC|GDC: co-press and co-sintering; LSCF: screen printing
	C2.	Ni-GDC | GDC | porous LSCF (infiltrated with LSCF, LSM, and SSC coatings)	
	C3.	Ni-YSZ anode | YSZ | GDC buffer layer| porous LSCF (blank cell without infiltration)	Ni-GDC|GDC: co-press and co-sintering; GDC and LSCF: screen printing
	C4.	Ni-YSZ anode | YSZ | GDC buffer layer| porous LSCF (infiltrated with LSCF, LSM, and SSC coatings)	
D.	**Cells provided by Delphi**		
	D1.	Ni-YSZ anode | YSZ | GDC buffer layer| porous LSCF (blank cell without infiltration)	
	D2.	Ni-YSZ anode | YSZ | GDC buffer layer| porous LSCF (blank cell with LSCF infiltration)	
	D3.	Ni-YSZ anode | YSZ | GDC buffer layer| porous LSCF (blank cell with LSM and SSC infiltration)	LSM infiltration: 0.0312mol/L solution in LSCF backbone

The experimental details are summarized as follows.

Preparation of electrolyte

Powders of YSZ and GDC ($Gd_{0.1}Ce_{0.9}O_{2-\delta}$) were either prepared in our lab using a glycine-nitrate process [10] or purchased from commercial sources. Electrolyte pellets were prepared by dry pressing. The typical pellets are about 100 μm thick with diameters of Φ10 mm and Φ13 mm. After sintering at 1450^{o}C for 5 hours, the densities of the sintered pellets were ~98 % of the theoretical value, as determined by the Archimedes's method.

Preparation of LSCF films by rf sputtering

For each electrolyte pellet, one side was ground and the other side was ground and polished using a MetPrep 3TM (Allied, High Tech Products, Inc.). The ground side was brush painted with $La_{0.6}Sr_{0.4}Co0_{.2}Fe_{0.8}O_{3-\delta}$ (LSCF) slurry, which was subsequently fired at 1080 for 2 hours to form a porous LSCF cathode of ~30 μm thick. Subsequently, a dense layer of LSCF was deposited on the polished side of the electrolyte by sputtering. The LSCF powder used for the LSCF slurry and for the LSCF targets was prepared by a citrate process.[9] To modify the surface catalytic properties of the LSCF, another thin film of LSM, SSC or YSZ were deposited on the top of the dense LSCF film electrode under various processing conditions to control the morphology, composition, and thickness.

Preparation of electrolyte-supported symmetrical cells with porous LSCF electrodes

Both sides of electrolyte pellets were first ground to plat. LSCF slurry was then screen-printed or brush painted on both sides of electrolytes and fired at 1080^{o}C for 2 hours. A platinum reference electrode was also printed/painted near the working electrode, and fired at 850^{o}C for 2 hours.

Preparation of anode-supported cells with porous LSCF cathodes

Powders of YSZ and GDC10 were prepared using a glycine-nitrate process [10]. The powders were fired at 800^{o}C and 600^{o}C for 2-4 h, respectively, to form the fluorite (YSZ, GDC) structure, as determined by X-ray diffraction analysis.

(a) Anode-supported cells with GDC electrolyte

NiO and GDC powders (NiO:GDC=65:35 wt.%) were pre-pressed under 50 MPa as substrate. The GDC powder and the substrate were then co-pressed at 250 MPa to form a green bi-layer and subsequently co-fired at 1350^{o}C in air for 5 h to densify the GDC film [11]. LSCF slurry was then screen printed or brush painted on the electrolyte, followed by firing at 1080^{o}C for 2 hours.

(b) Anode-supported cells with YSZ electrolyte

NiO and YSZ powders (NiO:YSZ=70:30 wt.%) were pre-pressed under 50 MPa as substrate. The YSZ powder and the substrate were then co-pressed at 250 MPa to form a green bi-layer and subsequently co-fired at 1425^{o}C in air for 5 h to densify the YSZ film. A thin GDC film was then screen printed or brush painted on the YSZ as a buffer layer to prevent the reaction between LSCF and YSZ. Subsequently, LSCF slurry was screen

printed or brush painted on the GDC buffer layer, followed by firing at 1080°C in air for 2 hours.[12]

Cells from Delphi

LSCF based button cells without cathode current collectors were received from Delphi Inc.. The electrode active area was 0.3 cm^2. Pt mesh was attached to cathode with Pt paste. The whole cell was mounted on an alumina supporting tube and the sealant was cured at 850^oC for 2 hours. Then the temperature was reduced to 825^oC and 700^oC for fuel cell testing using humidified hydrogen (3 vol% H_2O) as fuel and air as oxidant.

Preparation of LSM coatings

Aqueous nitrate solutions of LSM precursor with different concentration were prepared by mixing $La(NO_3)_3 \cdot 6H_2O$, $Sr(NO_3)_2$, $Mn(NO_3)_2 \cdot xH_2O$ and citric acid with corresponding molar ratios. Citric acid acted as a complex agent to form correct perovskite phase. Acetone was added into aqueous solution with a ratio of 1:1 (vol.%) to improve the wetting property on LSCF backbone. 6 µl of solution was then infiltrated into each side of porous LSCF electrode in symmetrical cell using micro-liter syringe in order to control the amount of loading. Meanwhile 3 µl of the same concentration solution was infiltrated into cathode of Delphi button cell. Vacuum apparatus was used to facilitate the penetration of the LSM solution into micro pores of LSCF. The infiltrated cells were fired at 850^oC for 2 hours to obtain the desired phase of LSM. For XRD characterization, identical nitrate solutions were also fired to powder under the same conditions. Blank cells without infiltration and cells infiltrated with LSCF solution were also tested for direct comparison.

Preparation of SSC coatings

Aqueous nitrate solutions of SSC precursor with different concentration were prepared by mixing $Sm(NO_3)_3 \cdot 6H_2O$, $Sr(NO_3)_2$, $Co(NO_3)_2 \cdot 6H_2O$ and citric acid with corresponding molar ratios. Citric acid acted as a complex agent to form correct perovskite phase. ethanol was added into aqueous solution with a ratio of 0.6:1 (wt.%) to improve the wetting property on LSCF backbone. 7µl of solution was then infiltrated into each side of porous LSCF electrode in symmetrical cell using micro-liter syringe in order to control the amount of loading. Vacuum apparatus was used to facilitate the penetration of the liquid into micro pores. The infiltrated cells were fired at 850^oC for 2 hour to obtain the desired phase of SSC. For XRD characterization, identical nitrate solutions were also fired to powder under the same conditions. Blank cells without infiltration and cells infiltrated with LSCF solution were also used for direct comparison.

RESULTS AND DISCUSSION

1. Design of Test Cells

We have designed a test cell using a buried LSCF layer as the current conductor. As schematically shown in Fig. 1 a), the berried LSCF has several functions. First, it is the current collector for the working electrode to minimize or eliminate the effect of sheet resistance; this becomes critical when the catalyst (LSM or SSC) layer is very thin. Second, it will not complicate the surface of LSM or SSC to be studied since it is buried under the catalyst layer without exposure to air. In contrast, the use of Pt strips or Pt paste on the top of the material to be studied may introduce other complications. Third, it also provides an ionic pathway (for oxygen vacancies) needed for the electrode reactions. If Pt strips are buried under the materials, Pt will block ionic transport and disturb the distribution of defects, resulting in non-uniform distribution of surface reactions and thus presence of surface transport. A highly active porous electrode will be used as the counter electrode (CE) and Pt mesh as current collector to minimize the impedance of the CE. Accordingly, the interfacial impedances, which can be readily separated from the impedance of the bulk processes by impedance spectroscopy, are dominated by the processes relevant to electrochemical reactions on the surface of LSM or SSC, thus providing us with a unique platform for investigations into the fundamental details of electrochemical reactions on the air-exposed surface.

The surface will be characterized very carefully using various state-of-the-art analytical tools to determine the surface species, phases, and surface morphologies, which will be correlated with the electrochemical performance under realistic operating environments.

One critical challenge in fabrication of these cells is the preparation of high quality films of LSCF and the new catalyst/electrode materials to be studied. We have developed some unique processes for deposition of high quality LSCF films on different substrates (e.g., Si, YSZ, and GDC). Shown in Fig 2 are cross-sectional and top views of a 200 nm thick LSCF film on Si, together with Raman spectra for phase confirmation (ordinary X-ray diffraction is insensitive to such a thin film).

2. Demonstration of surface limitations

Shown in Figure 2 are the interfacial polarization resistances of dense LSCF layers, as measured in the cell shown in Figure 1. Clearly, the polarization resistance decreases initially with the thickness of the LSCF layer until about 400 nm, implying that a minimum of 400 nm is needed to minimize the effect of sheet resistance. Further, the polarization resistance increased as the oxygen partial pressure was reduced, as shown in Figure 3, suggesting that it is the surface catalytic property, not the bulk transport property, that limits the performance of such a dense LSCF electrode. If it is limited by the ionic transport across the LSCF layer, the polarization resistance should decrease as the oxygen partial pressure is reduced since oxygen vacancy concentration and ionic conductivity are increased. Indeed, the electrode polarization resistance should decrease with the concentration of reactants (oxygen in this case).

3. Performance of cells with dense LSCF and LSM layers prepared by sputtering

Shown in Figure 4 are some typical impedance spectra of LSCF with/without LSM surface layer. Under open circuit conditions, the impedance of the LSCF with LSM is slightly smaller than the LSCF with a thin layer of LSM. When a DC polarization is imposed across the cell (-0.05 V), however, a reversal happened - the impedance of the LSCF with LSM become significantly smaller, suggesting a performance improvement by the

application of a thin layer LSM on LSCF. This represents a very interesting phenomenon. Our analysis using continuum models suggests that the much faster increase in catalytic activity of LSM over that of LSCF with the amplitude of cathodic polarization is due probably to the more dramatic change in oxygen vacancy concentration in LSM than in LSCF under polarized conditions. Additional experiments will be performed to validate this interpretation.

4. Performance of cells with SSC or LSM infiltrated porous LSCF electrodes

As seen in Figure 5, small particles of SSC are uniformly coated on the surface of LSCF. LSM catalyst film was uniformly coated on LSCF grains. The thickness of the film is about 20 nm, and the grain size of LSM varies from about 5 to 15 nm. Figure 6 shows some of the preliminary performances of LSCF backbone infiltrated with different concentrations of SSC. The electrode polarization resistances decreased with increasing concentration of SSC precursor solution. The performance of the LSCF backbone infiltrated with LSCF showed only slight improvement, suggesting that SSC infiltration has significantly improved the performance of LSCF due to its higher surface catalytic activity toward oxygen reduction.

Similar performance improvement has also been observed on LSCF infiltrated with LSM under polarized conditions. Shown in Figure 7 are the polarization resistances of LSCF infiltrated with 0.125 M $L_{0.85}S_{0.15}MnO_3$ (LSM). While the polarization resistance of the LSCF infiltrated with LSM is higher than that of the LSCF without LSM infiltration under OCV conditions, the former decreased with the amplitude of cathodic polarization much faster than the latter, suggesting that the catalytic activity of LSM is electrically activated under a DC polarization. This is consistent with the behavior of LSM commonly reported in the literature: the catalytic activity of LSM toward oxygen reduction increases with increasing DC polarization. More systematic studies on the effect of thickness, morphology, and composition of the LSM coatings on LSCF cathodes are needed in order to gain further insight into the mechanism of performance enhancement.

5. Preliminary stability data (~100 hours)

The stability and performance of test cells with LSCF cathodes infiltrated with LSM and SSC have been tested for about 100 hrs at 700^{o}C and 825^{o}C. Figure 8 are impedance spectra of LSCF symmetrical cell with or without infiltrated LSM and SSC before/after 100 hours operation at 700^{o}C and 825^{o}C. Each spectrum was collected about 1 hour after the cell reached a steady state. Bulk resistances of these cells were all close to theoretical values. In order to clearly show the polarization resistances of the electrodes, all bulk resistances were subtracted from the total impedances of the cells; thus, the impedance spectra presented correspond to the interfacial polarization impedances of the cells.

As shown in Figure 8 (a) and 9 (a) for testing at 700^{o}C, blank LSCF electrodes (without infiltration) exhibited an area specific (interfacial polarization) resistance of 0.430 Ω-cm^2, which was reduced to 0.228 Ω-cm^2 and 0.101 Ω-cm^2 by LSM and SSC infiltration, respectively. The observed increase in performance enhancement is due primarily to the increase in catalytic activity and in electrode surface area by the LSM and SSC coatings. After 100 hours operation, the performances of the blank cell degraded quickly, and so was the LSM infiltrated cell. However, the SSC infiltrated cell appeared to be more stable at low temperatures.

As shown in Figure 8 (b) and 9 (b) for testing at 825^{o}C, blank LSCF cell had an interfacial resistance of 0.184 Ω-cm^2, which was reduced to 0.073 Ω-cm^2 and 0.013 Ω-cm^2 by the infiltration of LSM and SSC, respectively. This is due mainly to the increase in surface catalytic activity and potentially to increased electrode surface area. After 100 hours operation, the total resistance of the blank LSCF cell increased by ~10%, while those of the LSM and SSC infiltrated cells showed little degradation in performance. In addition to the improvements in stability, LSM and SSC infiltration seems to increase the surface catalytic activity and this reduce the polarization resistance. One possible explanation is that vacancy transport through the thin film coating and small particles of LSM and SSC were sufficiently fast at high temperatures (in contrast to the data collected at 700C where mass transfer may limit the performance of the cells).

Shown in Figure 10 are the cell voltages of two delphi cells with/without LSM infiltration as a function of time under a constant current of 0.25 A at 825 ^{o}C. The cell infiltrated with LSM showed higher terminal voltage and better stability compared with the blank cell without LSM infiltration. The corresponding I-V curves and power output characteristics are shown in Figure 11, showing a higher power output of the cell with LSM infiltration both before and after the stability test for 100 hrs.

6. Performance of YSZ coated LSCF prepared by sputtering

In addition to LSM and SSC, a thin film of YSZ coating was also applied to the surfaces of LSCF to evaluate the effect of YSZ on the surface properties. Schematically shown in Figure 12 is a cross-sectional view of the cells used for this study. GDC pellets were used as the electrolytes. A highly porous LSCF layer (with Pt mesh) was used as the counter electrode for the electrochemical measurements. A dense LSCF layer of 1 micron was deposited on the other side of the GDC electrolyte by rf sputtering, to which a thin coating of YSZ was deposited by reactive sputtering. The thickness of the YSZ layer is about 4 nm and believed to be continuous. The performance was characterized and compared with a blank cell with a dense LSCF electrode without YSZ coating.

Shown in Figure 13 is the dependence of polarization resistance on overpotential at 700 and 800ºC. It was found that samples of YSZ coated LSCF have higher resistances than the LSCF without YSZ coating. The increase in polarization resistance becomes more pronounced at higher over-potentials and at higher temperatures.

Shown in Figure 14 is some typical impedance spectra of the samples with or without YSZ coating acquired at different temperatures with 0.1 or 0.5 V dc polarization. Analysis of the impedance spectra suggests that the impedance arcs in the medium frequency range (MF) for the YSZ-coated LSCF is significantly greater than those for the blank LSCF without YSZ. This seems to imply that the YSZ coating influences the electrochemical process occurred in the medium frequency range, likely associated with blocking of some reaction sites on LSCF by YSZ.

CONCLUSIONS

Under the support of this project, we validated the hypothesis that the *performance* and *stability* of a porous LSCF cathode may be improved by the application of a catalytically active coating though infiltration. The selection of the catalytic materials as well as the detailed microstructures of the porous LSCF and the catalyst layer may critically impact the performance of the proposed cathodes.

We have successfully developed a platform for reliably evaluating the surface catalytic properties of cathode materials.

It is confirmed that the surface catalytic activity limits the performances of LSCF-based cathodes. The polarization resistances decreased initially with the thickness of the LSCF layers until about 400 nm, implying that a minimum of 400 nm is needed to minimize the effect of sheet resistance. Further, the polarization resistance increased as the oxygen partial pressure was reduced, suggesting that it is the surface catalytic property (not the bulk transport property) that limits the performance of such a dense LSCF electrode. If it is limited by the ionic transport across the LSCF layer, the polarization resistance should decrease as the oxygen partial pressure is reduced since oxygen vacancy concentration and ionic conductivity are increased. Indeed, the electrode polarization resistance should decrease with the concentration of reactants (oxygen in this case).

Also, the stability and performance of LSCF-based cathodes have been enhanced by infiltration of a catalytically active coating. The polarization resistance (R_P) of LSCF cathodes infiltrated with different concentrations of SSC, as determined using impedance spectroscopy, decreased with the concentration of SSC precursor solution. The performance of the LSCF backbone infiltrated with LSCF showed only slight improvement, suggesting that SSC infiltration has significantly improved the performance of LSCF due to its higher surface catalytic activity toward oxygen reduction.

However, many details are yet to be determined. For example, it is not clear how the surface morphology, composition, and thickness of the coatings change under operating conditions, how these changes influence the electrochemical behavior of the cathodes, and how to control the microscopic details of the coatings in order to optimize the performance; .

Further, it is not clear why the degradation rates of LSCF cathodes are relatively high, why a LSM coating improves the stability of LSCF cathodes, which catalyst would be the most effective one for LSCF or which more conductive matrixes would be a better backbone than LSCF. The long-term stability of the interfaces (e.g., LSM/LSCF) is yet to be investigated as well.

Figures

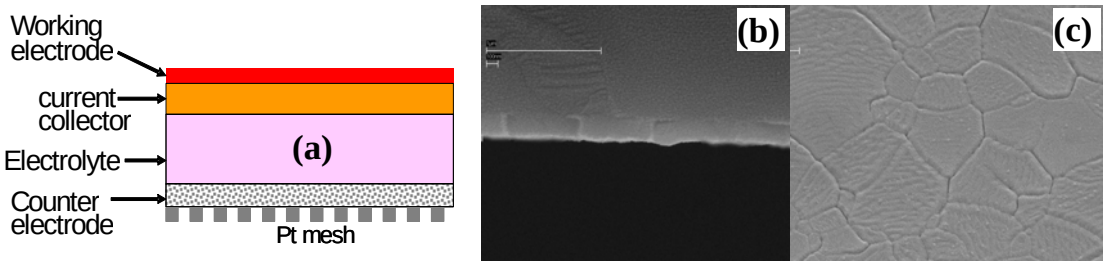

Figure 1. (a) Schematic of a test cell for study of the air-exposed surface of LSM or SSC. **(b)** a cross-sectional and **(c)** a top view of an LSCF film, prepared by magnetron sputtering on a Si substrate kept at 300˚C at a working pressure of 2.2×10^{-2} mbar Ar. The LSCF film was about 200 nm thick. The average grain size is ~1 μm after annealing at 700˚C for 30 min.

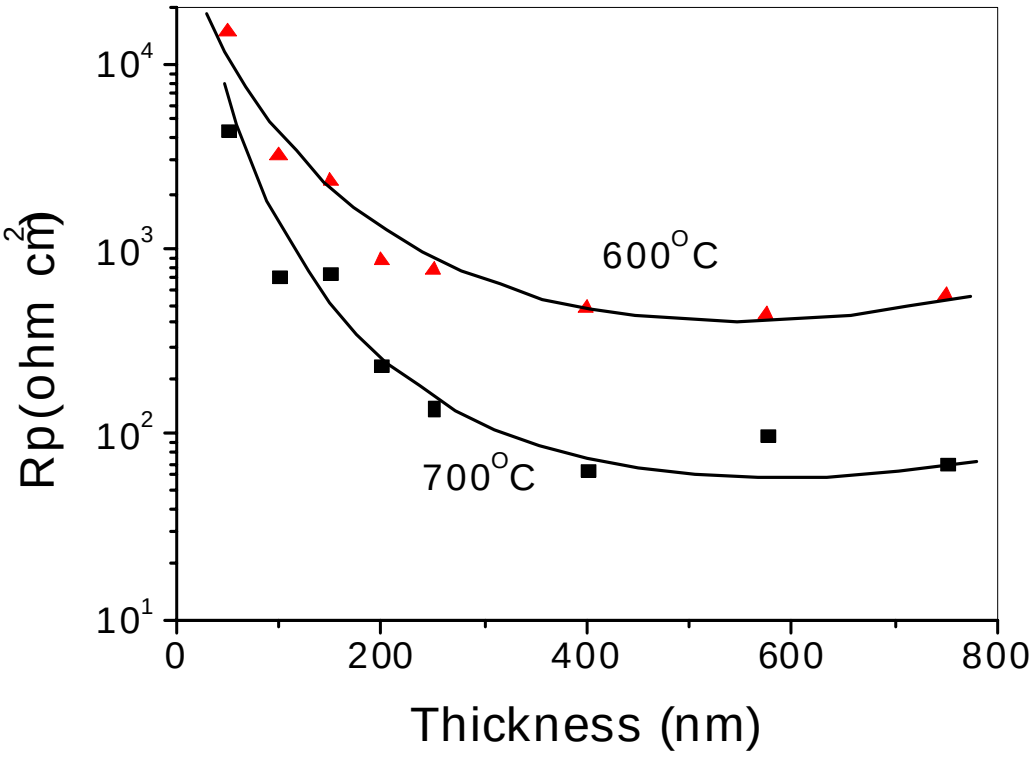

Figure 2. Polarization resistances of dense LSCF electrodes of different thickness (prepared by sputtering) as measured in a cell shown in Figure 1 at 600 and 700ºC.

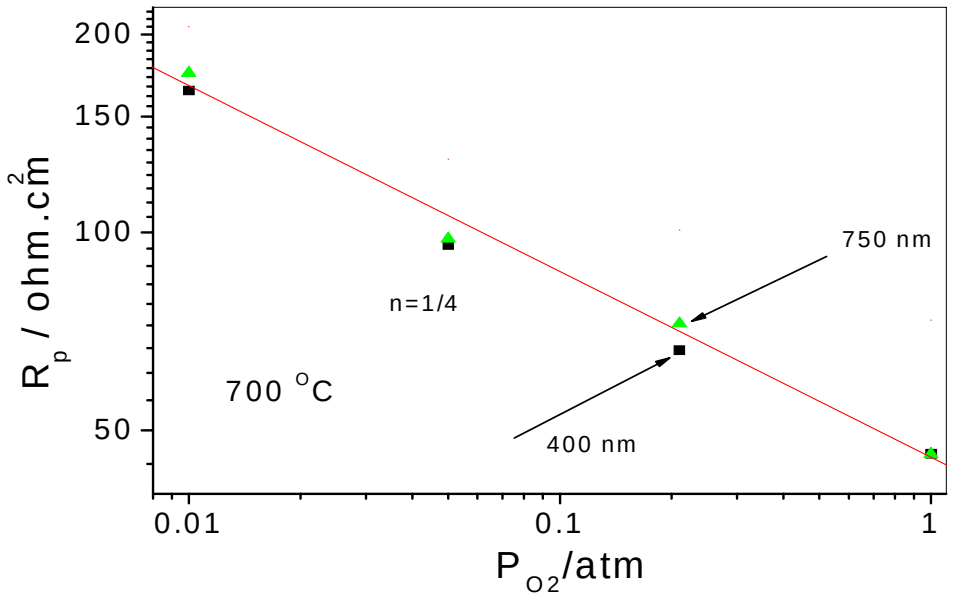

Figure 3. The polarization resistances of dense LSCF electrodes (with a thickness of 400 nm and 700 nm) as measured in a cell shown in Figure 1 at 700 ^{O}C in different partial pressures of oxygen.

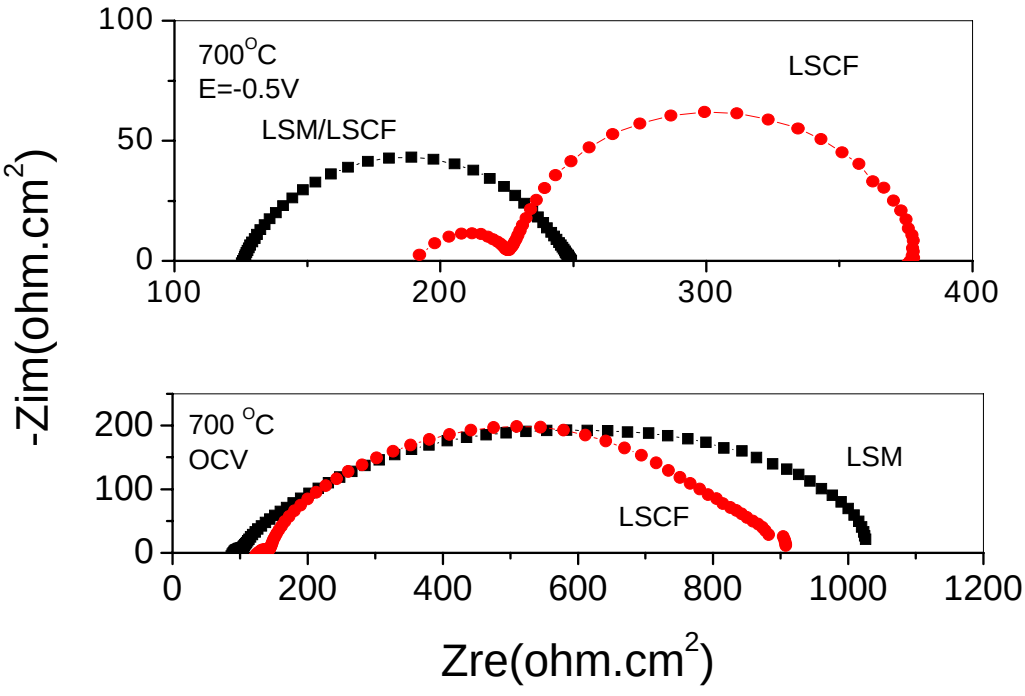

Figure 4. The impedance spectra measured at 700^{O}C in air at OCV and under –0.5 V cothodic polarization of a 150 nm thick LSCF electrode with or without an LSM coating.

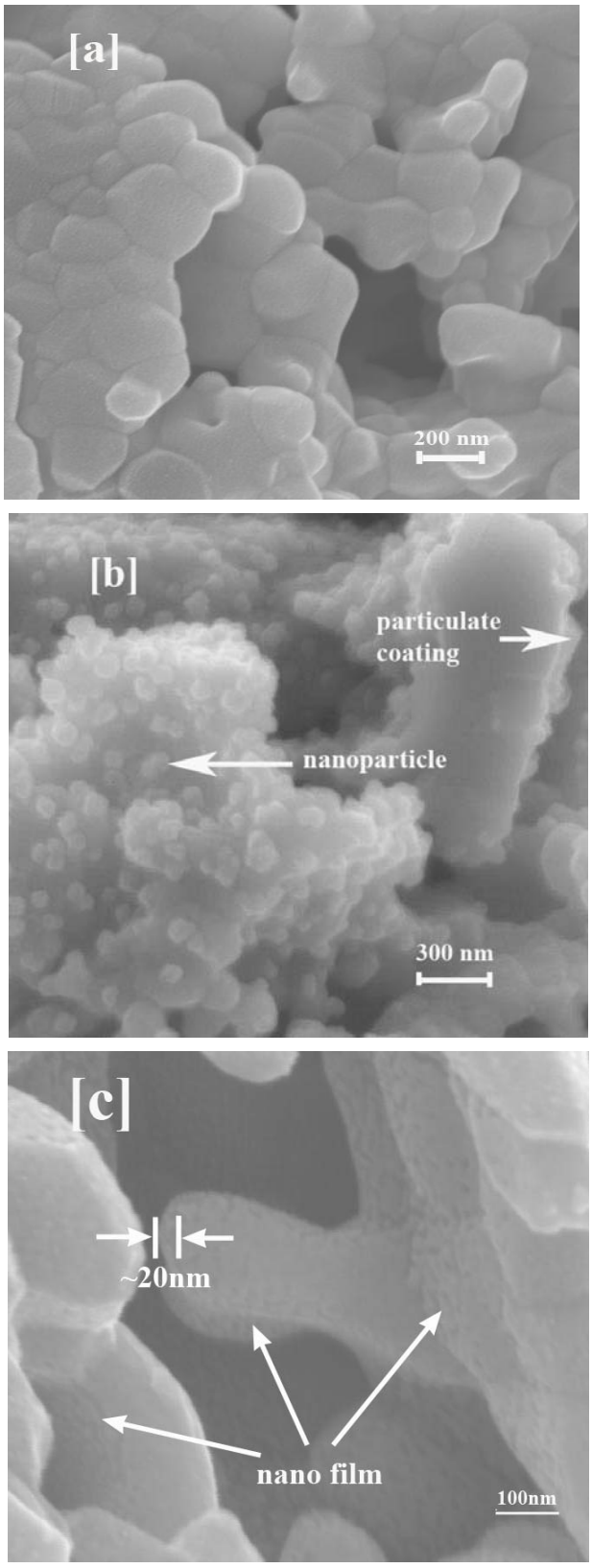

Figure 5. Cross-sectional views of porous LSCF cathodes: (a) blank LSCF, (b) infiltrated with SSC (concentration of SSC solution: 1.44 mol/L), and (c) infiltrated with LSM (concentration of LSM solution: 0.0312 mol/L).

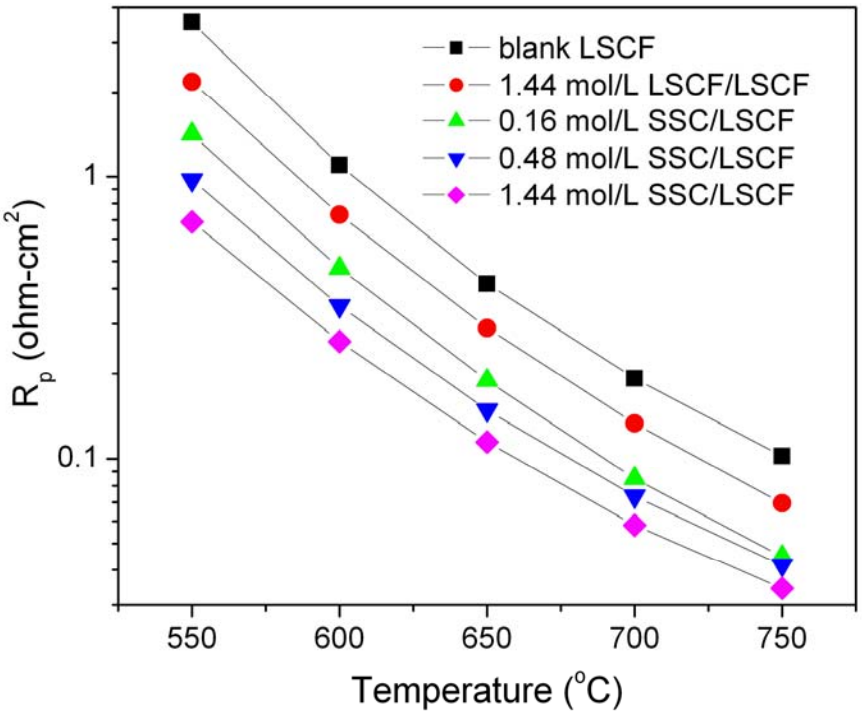

Figure 6. Electrode polarization resistances of porous LSCF electrodes infiltrated with different concentrations of SSC (compared with those of a blank LSCF electrode without infiltration).

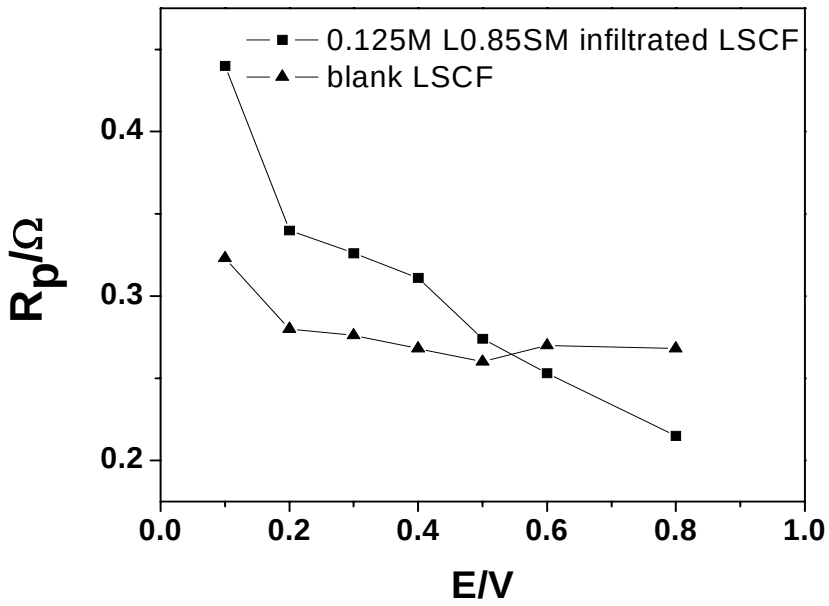

Figure 7. Electrode polarization resistances (R_p) of an LSCF cathode with and without infiltration of 0.125 mol/L LSM, as measure at 700^{O}C in air.

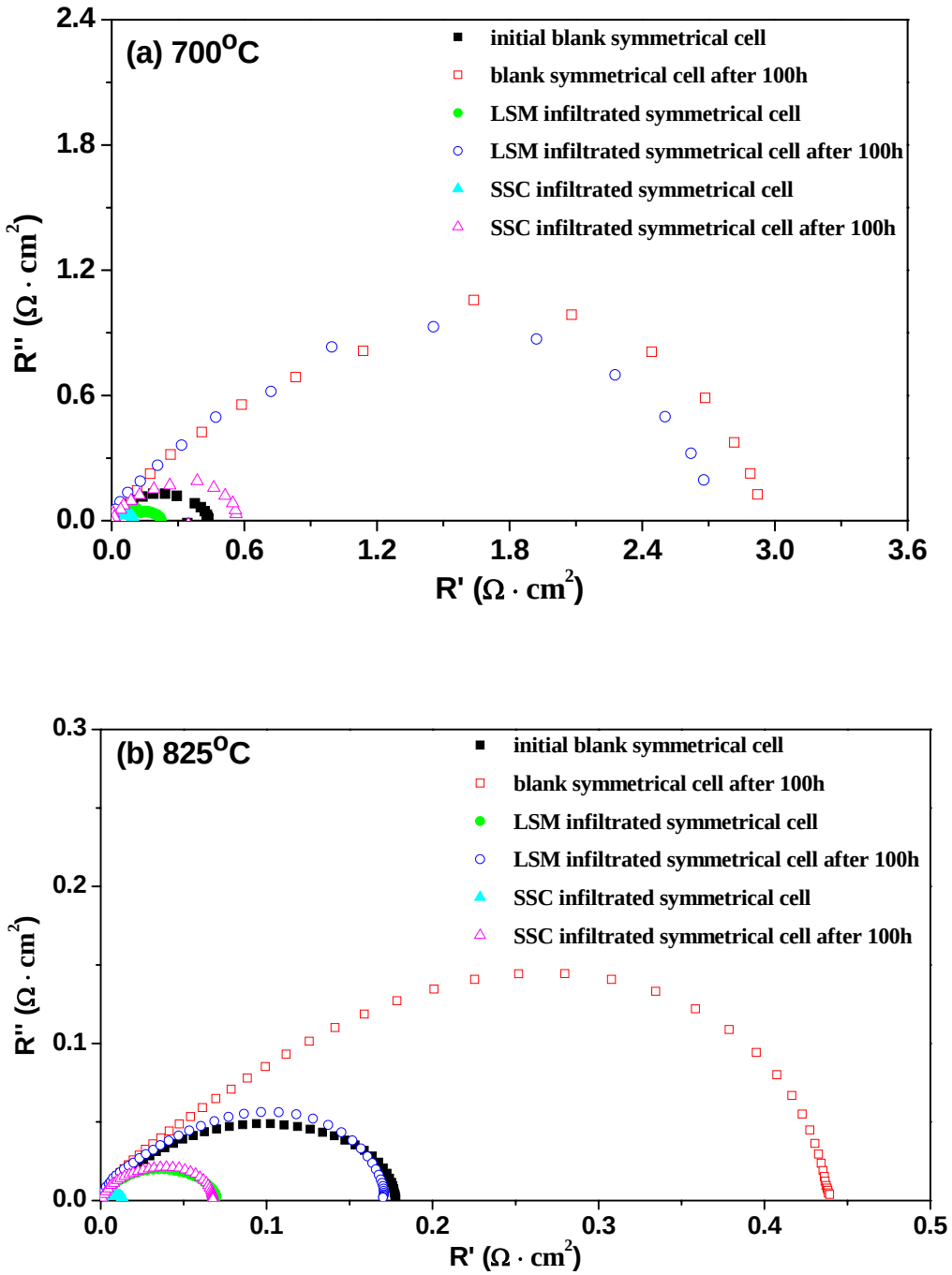

Figure 8. Impedance spectra of LSCF cathodes with/without infiltrated LSM and SSC before/after 100 hours operation at (a) 700°C and (b) 825°C, as measured in a symmetrical cell with configuration of porous LSCF | GDC| porous LSCF.

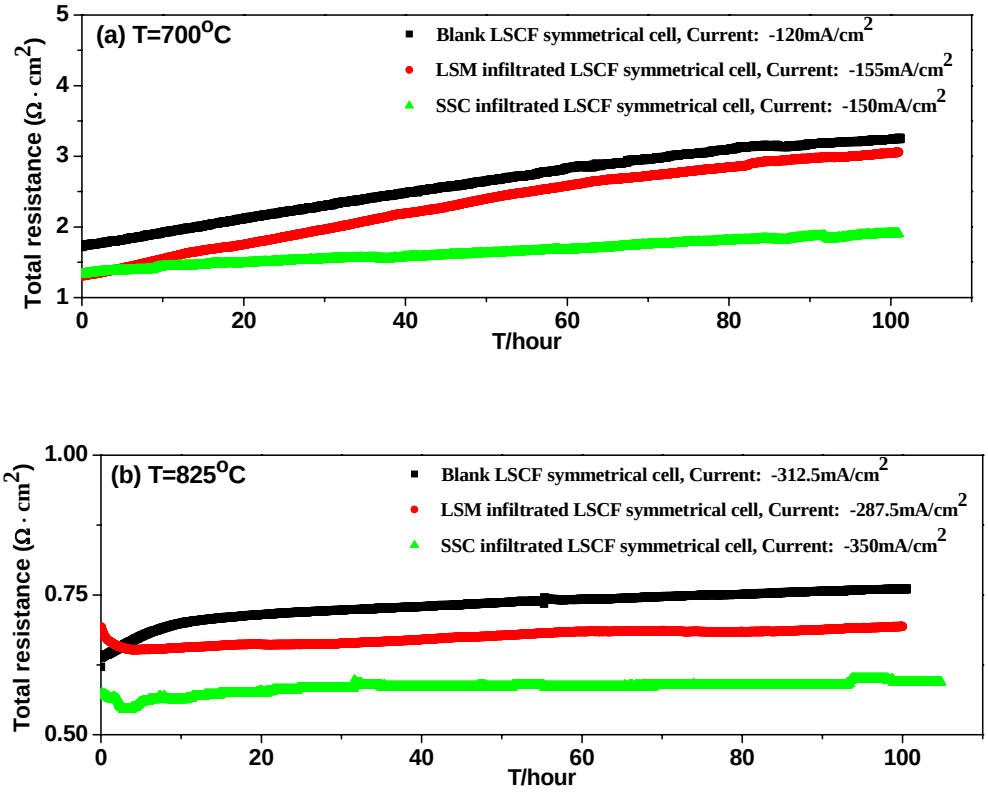

Figure 9. Total resistances of symmetrical cells with/without an infiltrated LSM or SSC coating for 100 hours operation at (a) 700°C and (b) 825°C.

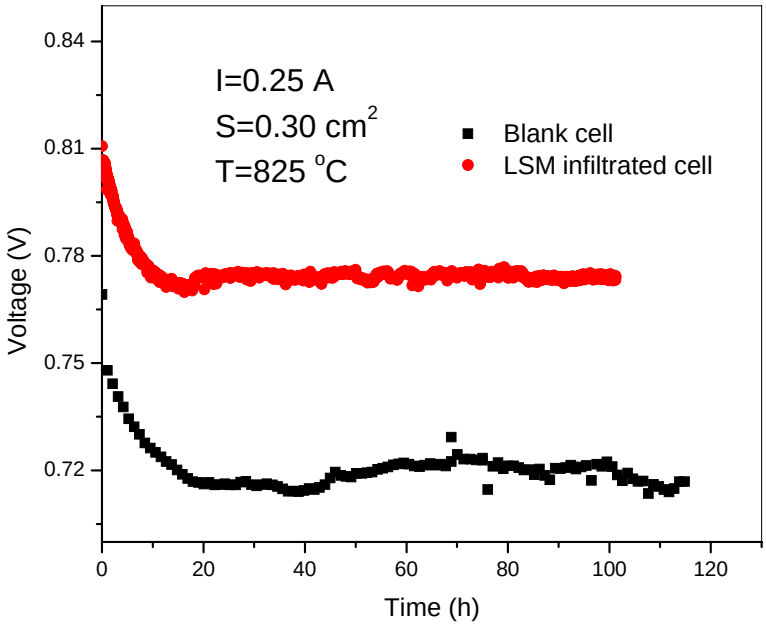

Figure 10. Terminal voltages of test cells with LSCF cathodes with and without infiltration of 0.0312 M LSM as measured under a constant current of 0.25 A at 825 °C.

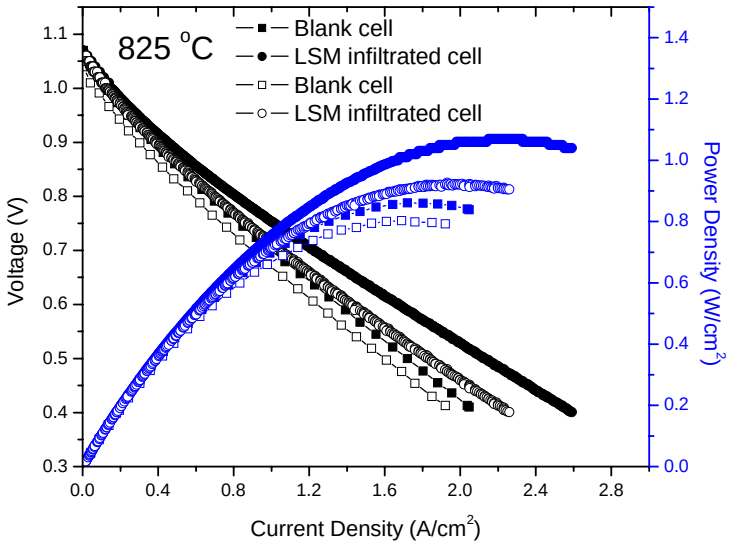

Figure 11. Current-voltage (I-V) curves and power output characteristics of the two test cells based on LSCF cathodes infiltrated with LSM before and after a stability test for 100 hours.

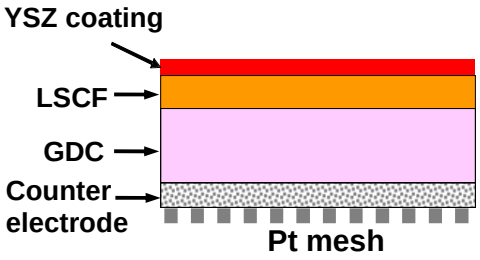

Figure 12. Schematic of the test cell with a dense LSCF electrode covered by a thin YSZ film, prepared by sputtering.

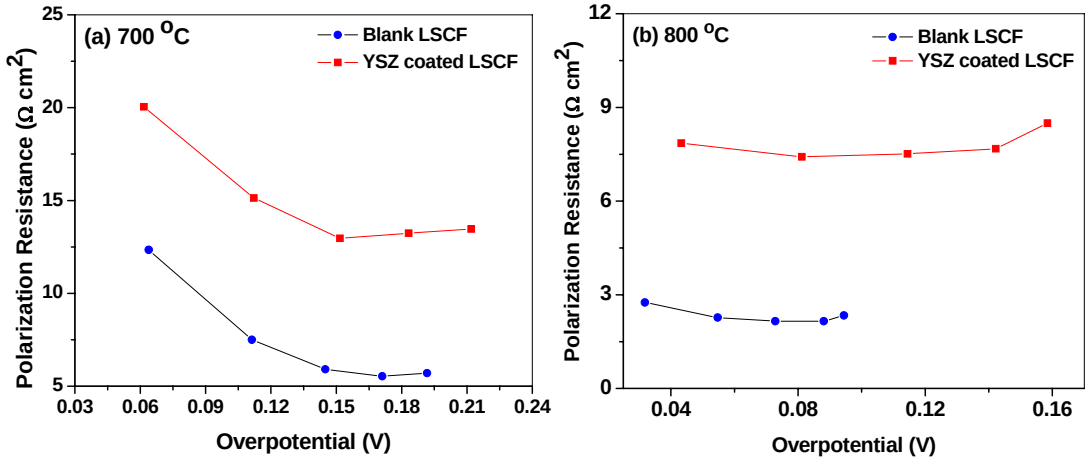

Figure 13. Polarization resistance as a function of over-potential applied to the cell at (a) 700°C and (b) 800°C.

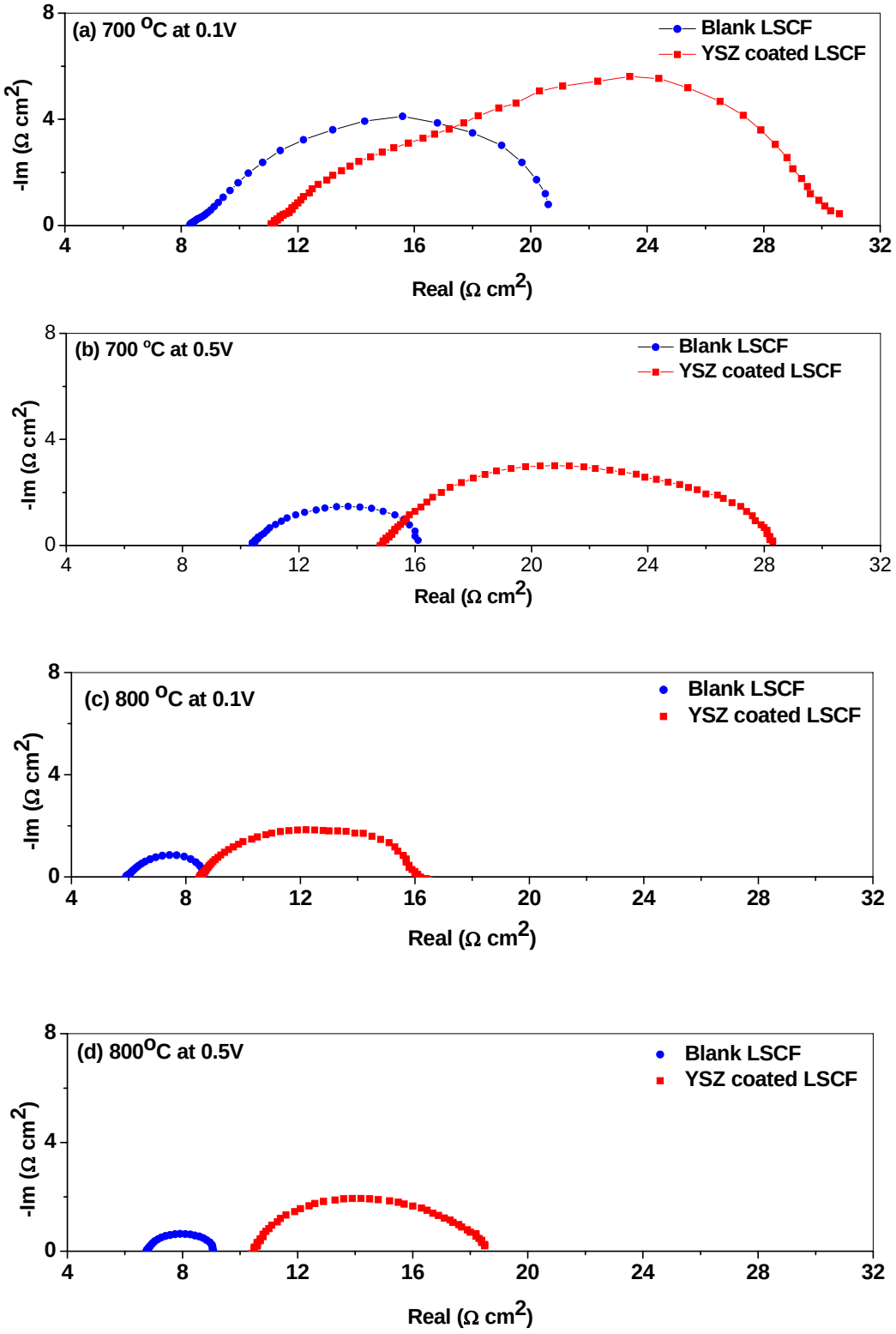

Figure 14. Impedance spectra for cells with dense LSCF electrodes with or without a thin coating of SZ measured at 700 and 800ºC under a dc polarization of 0.1 or 0.5 V.

REFERENCES

1. S. Shaffer. Development update on Delphi's solid oxide fuel cell power system. Technical report, Delphi Corporation, 2006.
2. Erica Perry Murray, Tespin Tsai, Scott A. Barnett, "Oxygen transfer processes in (La,Sr)MnO, /Y_2O_3-stabilized ZrO_2 cathodes: an impedance spectroscopy study", Solid State Ionics, 110: 235-243, 1998
3. Steele, B. C. H.; Heinzel, A. "Materials for fuel-cell technologies", *Nature, 414*: 345, 2001
4. S. P. Simner, M. D. Anderson, M. H. Engelhard, and J. W. Stevenson, "Degradation Mechanisms of La–Sr–Co–Fe–O SOFC Cathodes", Electrochemical and Solid-State Letters, 9(10) A478-A481, 2006.
5. S. J. Benson, D. Waller, and J. A. Kilner, "Degradation of $La_{0.6}Sr_{0.4}Fe_{0.8}Co0._2O_{3-\delta}$ in Carbon Dioxide and Water Atmospheres", Journal of The Electrochemical Society, 146 (4) 1305-1309, 1999
6. F. Tietz, V.A.C. Haanappel, A. Mai et al. "Performance of LSCF cathodes in cell tests", Journal of Power Sources 156 (2006) 20–22
7. D. Mebane, M. Liu, L. Wilson, W. Surdoval, "Novel cathode design for solid oxide fuel cells using particle infiltration technology"**,** Provisional Patent Application, April 2007.
8. T. Z. Sholklapper, C. Lu, C. P. Jacobson, S. J. Visco, and L. C. De Jonghe. "LSM-infiltrated solid oxide fuel cell cathodes". Electrochemical and Solid-State Letters, 9(8):A376–A378, 2006.
9. Z. Liu, M. F. Han and W. T. Miao , Journal of Power Sources, 173 (2): 837-841 2007
10. C. R. Xia and M. L. Liu, "ow-temperature SOFCs based on $Gd_{0.1}Ce_{0.9}O_{1.95}$ fabricated by dry pressing", solid State Ionics, 144, 249 (2001)
11. Shaowu Zha, Ashley Moore, Harry Abernathy et al. "GDC-Based Low-Temperature SOFCs Powered by Hydrocarbon Fuels", Journal of The Electrochemical Society, 151 (8): A1128-A1133, 2004
12. S.P. Simner, J.F. Bonnett, N.L. Canfield et al. "Development of lanthanum ferrite SOFC cathodes", Journal of Power Sources, 113: 1–10, 2003